Supplemental Material for: Revealing the spectral response of a plasmonic lens using low-energy electrons

Shuiyan Cao,[1] Eric Le Moal,[1,*] Florian Bigourdan,[2] Jean-Paul Hugonin,[2] Jean-Jacques Greffet,[2] Aurélien Drezet,[3] Serge Huant,[3] Gérald Dujardin,[1] and Elizabeth Boer-Duchemin[1]

[1] *Institut des Sciences Moléculaires d'Orsay (ISMO), CNRS, Univ Paris Sud, Université Paris-Saclay, F-91405 Orsay (France)*

[2] *Laboratoire Charles Fabry, Institut d'Optique, 91127 Palaiseau, France*

[3] *Université Grenoble Alpes, Institut NEEL, F-38000 Grenoble, France and CNRS, Institut NEEL, F-38042 Grenoble, France*

(Dated: August 30, 2017)

In this supplementary material, experimental spectra of the light emitted upon STM excitation of single circular slits and generated data confirming the role of SPP cavity modes are shown. In addition, the procedure for correcting experimental spectra for the detection efficiency of our setup is explained.

PACS numbers: 73.20.Mf, 68.37.Ef

CAVITY MODES IN SINGLE-CIRCULAR-SLIT PLASMONIC LENS

Figure S1(a) shows optical spectra measured for different single-circular-slit plasmonic lenses using configuration 2 of the experimental setup discussed in the article. The spectra shown in Fig. S1(a) differ from that of an unstructured thin gold film; they exhibit peaks and dips. When varying the inner diameter D, the peaks and dips shift in energy; therefore, it is unlikely that these features are due to resonances inside the gap of the slit (the slit width W is always the same). Whispering-gallery modes, i.e., guided surface plasmon polariton (SPP) waves propagating along the circular trajectory at the slit edges or in the gap, can be discarded as well: the axial symmetry of the system, when the tip is centered on the plasmonic structure, and the out-of-plane orientation of the source dipole do not allow the excitation of these modes. Thus, we infer that the features seen in Fig. S1(a) are related to the cavity modes of the plasmonic structure, i.e., SPP standing waves formed due to SPP reflection at the circular slit back to the center of the structure.

In order to confirm the origin of the features observed in the experimental spectra, we compare them to "generated" data shown in Fig. S1(b). This generated data is obtained in the following way using a simple model illustrated in Fig. S2. The SPP source produces a discontinuity A^i that can be easily calculated using the principle of reciprocity, provided that the mode is properly normalized[S1]. With the notations introduced in Fig. S2(b), where r is the complex amplitude reflection coefficient at the cavity boundary and k_{sp} is the SPP wavevector, the field at the source location satisfies the following system of equations.

$$\begin{cases} A^+ = rA^- \exp\left(ik_{sp}D\right) + A^i \\ A^- = rA^+ \exp\left(ik_{sp}D\right) + A^i \end{cases} \tag{S1}$$

which may be rewritten as follows:

$$\begin{cases} A^+ - A^- = r(A^- - A^+) \exp\left(ik_{sp}D\right) \\ A^- + A^+ = r(A^+ + A^-) \exp\left(ik_{sp}D\right) + 2A^i \end{cases} \tag{S2}$$

Thus, the field at the source location reads:

$$A^+ = A^- = \frac{A^i}{1 - r \exp\left(ik_{sp}D\right)} \tag{S3}$$

The generated data shown in Fig. S1(b) corresponds to the featureless spectrum measured upon STM excitation of SPPs on an unstructured thin gold film, spectrally weighted by the squared modulus of the electric field calculated using Eq. S3 for D = 3, 4, 5 and 6 μm. In the model, we find that $|r| = 0.04$ and $\arg r = \pi$ best fit the experimental data. The asterisks indicating the spectral position of the peaks in Fig. S1(a) are reproduced in Fig. S1(b) in order to highlight the agreement between the generated and experimental data.

The model used above is very simplistic since it does not describe the out-of-plane SPP-to-photon scattering at the slit; nevertheless, the generated data reproduces the number of peaks, their spectral position and spectral width quite well. The main discrepancy is that the model underestimates the low energy region of the spectrum, which may be due to the frequency-dependent SPP scattering efficiency at the slit. All together, these observations confirm the role played by the cavity modes of the central disk in the spectral response of a single-circular-slit plasmonic lens upon STM-excitation.

SPECTRUM CORRECTION FOR DETECTION EFFICIENCY

The spectra shown in the article are corrected for the spectral response of the setup. After subtracting a background reference measured with no light, the experimental data are simply divided by the detection efficiency

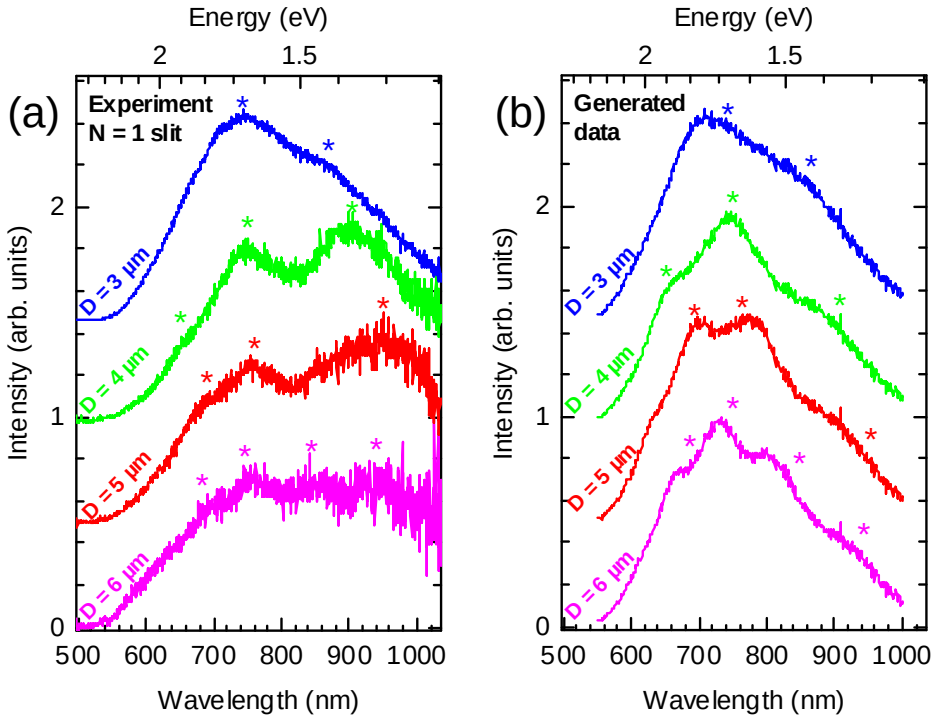

FIG. S1. Electrical excitation of a single-circular-slit plasmonic lens: the effect of the inner diameter on the spectrum. (a) Spectral distribution of the light emitted upon STM excitation of a single- (N = 1) circular-slit plasmonic lens of different inner diameters D, etched in a 200-nm gold film on glass. All spectra are corrected for the spectral response of the instrument, which includes the transmission of the microscope objective, the scattering efficiency of the diffraction grating and the quantum efficiency of the CCD camera used in the spectrometer (the spectra are vertically offset for clarity). The STM bias is U_b = 2.8 V, the current setpoint is I_t = 3 to 4 nA and the acquisition time is 300 s. (b) Generated spectra, obtained by multiplying two terms: (i) the squared modulus of the electric field theoretically produced by a point source in an SPP cavity of length D and (ii) the experimental data measured on a thin (50 nm) unstructured gold film (data shown in Fig. 5b). The electric field in the SPP cavity is calculated using a simple model described in the text, where the SPP source is located at the center of the cavity. In this model, we use the leakage radiation spectrum measured on the thin gold film as the power spectrum of the SPP source (this is why the generated data shown in panel b exhibits experimental noise).

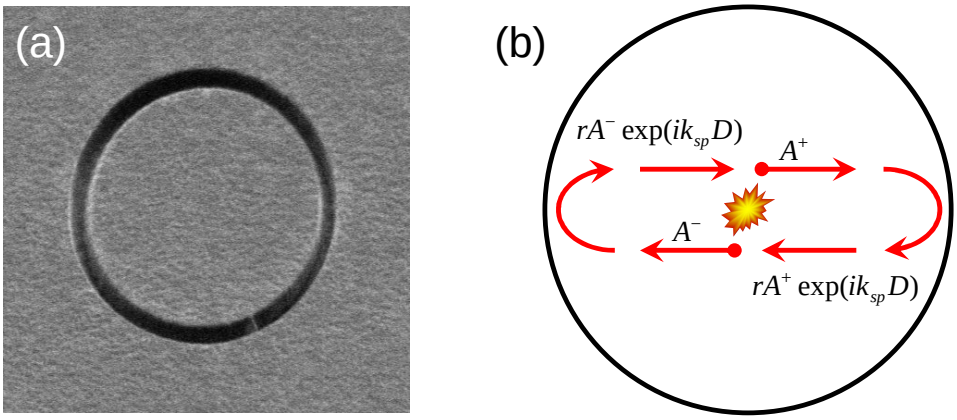

FIG. S2. (a) Scanning electron micrograph of a single-circular-slit plasmonic lens of diameter D = 5 μm and (b) schematic explanation of the model used to calculate the electric field produced by a point source in an SPP cavity.

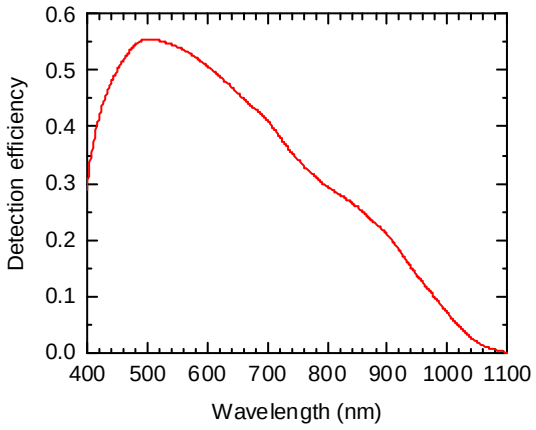

FIG. S3. Data used to correct the experimental spectra for the frequency-dependent detection efficiency of our setup. Here, the detection efficiency is obtained from the product of the transmission coefficient of the microscope objective, the diffraction efficiency of the grating and the quantum efficiency of the CCD camera.

plotted in Fig. S3. The data shown in Fig. S3 are calculated by multiplying the transmission coefficient of the microscope objective with the first-order diffraction efficiency of the diffraction grating used in the spectrometer and the quantum efficiency of the CCD camera. These technical data are obtained from the equipment vendors and are interpolated to match the wavelength sampling used in the experiment. Here, the detection efficiency is *relative* (not *absolute*), since it does not taken into account the collection efficiency of the objective lens, which is limited by its angular aperture.

* eric.le-moal@u-psud.fr

[S1] J. P. Hugonin and P. Lalanne, J. Opt. Soc. Am. A **22**, 1844 (2005).